



Audio Engineering Society Convention Paper

Presented at the 135th Convention
2013 October 17–20 New York, USA

This Convention paper was selected based on a submitted abstract and 750-word precis that have been peer reviewed by at least two qualified anonymous reviewers. The complete manuscript was not peer reviewed. This convention paper has been reproduced from the author's advance manuscript without editing, corrections, or consideration by the Review Board. The AES takes no responsibility for the contents. Additional papers may be obtained by sending request and remittance to Audio Engineering Society, 60 East 42nd Street, New York, New York 10165-2520, USA; also see www.aes.org. All rights reserved. Reproduction of this paper, or any portion thereof, is not permitted without direct permission from the Journal of the Audio Engineering Society.

Simulation of an analog circuit of a wah pedal: a port-Hamiltonian approach

Antoine Falaize-Skrzek¹, and Thomas H  lie¹

¹IRCAM, Paris, 1 place Igor Stavinsky, 75004, France

Correspondence should be addressed to Antoine Falaize-Skrzek (falaize@ircam.fr)

ABSTRACT

Several methods are available to simulate electronic circuits. However, for nonlinear circuits, the stability guarantee is not straightforward. In this paper, the approach of the so-called "Port-Hamiltonian Systems" (PHS) is considered. This framework naturally preserves the energetic behavior of elementary components and the power exchanges between them. This guarantees the passivity of the simulations.

1. INTRODUCTION

Several methods (Wave Digital Filter [1], Nodal DK method [2], etc.) are available to simulate electronic circuits. However, for nonlinear circuits, the stability guarantee is not straightforward. In this paper, the approach of the so-called "Port-Hamiltonian Systems" (PHS) is considered. This framework naturally preserves the energetic behavior of elementary components and the structure of power exchanges between them, leading to passive modeling. PHS have been introduced in the 1990's [4, 5, 6]. They correspond to open dynamical systems made of energy storage components, dissipative components, and some connection ports through which energy can transit.

The method is applied to the CryBaby wah pedal circuit, which involves nonlinear and time-varying components (see *e.g.* [7] for simulation based on the Nodal DK approach).

A short introduction to PHS is given in section 2. The CryBaby's circuit is presented in section 3. Its network is analysed within the graph theory framework, and a dictionary of its elementary components is given. In section 4, these elements are used to derive a PHS corresponding to this circuit. Section 5 is concerned with the derivation of a numerical scheme which is designed to preserve the power balance. Finally, simulation results are presented in section 6.

2. PORT-HAMILTONIAN SYSTEMS: BASICS AND INTRODUCTORY EXAMPLE

2.1. Formalism

Consider an electronic circuit composed of:

n_S **storage components**, energy of which is $\mathfrak{E}_s = h_s(x_s) \geq 0$, (typically, for a capacitance C , the state and the positive definite function can be the charge $x = q$ and $h(q) = q^2/(2C)$);

n_D **dissipative components**, for which the dissipated power is $\mathcal{D}_d = \mathcal{D}_d(w_d) \geq 0$ (typically, for a standard resistance R , w can be a current $w = i$ and $\mathcal{D}(i) = R \cdot i^2$);

n_P **external ports**, with incoming power \mathcal{P}_p .

Denoting voltages v and currents i in *receiver convention*, the power *received* by a dipole is given by the product $v \cdot i$. For storage components, these quantities are related to $\frac{dx_s}{dt}$ and $\frac{dh_s}{dx_s}$ in some way, as their product is precisely the *received power* ($v_s \cdot i_s = \frac{d\mathfrak{E}_s}{dt} = \frac{dh_s}{dx_s} \cdot \frac{dx_s}{dt}$): for the capacitance, these *constitutive laws* are $i = dq/dt = dx/dt$ and $v = q/C = dh/dq$. A similar mapping of quantities is provided for dissipative components, based on the factorization $\mathcal{D}_d(w_d) = w_d \cdot z_d(w_d)$: for the resistance, $i = w$ and $v = R \cdot i = z(w)$. For external ports, we arrange voltages v_p and currents i_p in two vectors: one is considered as an input u_p and the other one as the associated output y_p so that $\mathcal{P}_p = y_p \cdot u_p$.

The linear relations fulfilled by all the voltages and the currents due to the connection of components are derived by applying Kirchhoff's laws to the network of the circuit (see § 3.1 and [7]). Combining these relations and *constitutive laws* provides the equations that governs the circuit. These equations have the form of a so-called *Port-Hamiltonian System* (PHS) [6, eq 2.53]:

$$\begin{pmatrix} \frac{dx}{dt} \\ \mathbf{w} \\ \mathbf{y} \end{pmatrix} = \begin{pmatrix} \mathbf{J}_x & -\mathbf{K} & \mathbf{G}_x \\ \mathbf{K}^T & \mathbf{J}_w & \mathbf{G}_w \\ \mathbf{G}_x^T & \mathbf{G}_w^T & \mathbf{J}_y \end{pmatrix} \cdot \begin{pmatrix} \nabla \mathcal{H}(\mathbf{x}) \\ \mathbf{z}(\mathbf{w}) \\ \mathbf{u} \end{pmatrix}, \quad (1)$$

where matrices \mathbf{J}_x , \mathbf{J}_w , \mathbf{J}_y are skew-symmetric. $\nabla \mathcal{H} : \mathbb{R}^{n_S} \rightarrow \mathbb{R}^{n_S}$ denotes the gradient of the total energy $\mathfrak{E} = \mathcal{H}(\mathbf{x}) = \sum_{s=1}^{n_S} h_s(x_s)$ w.r.t. the vector of the

states $[\mathbf{x}]_s = x_s$. Function $\mathbf{z} : \mathbb{R}^{n_D} \rightarrow \mathbb{R}^{n_D}$ denotes the collection of functions z_d w.r.t. the vector $\mathbf{w} \in \mathbb{R}^{n_D}$ of $[\mathbf{w}]_d = w_d$ so that $\mathbf{z}(\mathbf{w})^T \cdot \mathbf{w} = \sum_{d=1}^{n_D} \mathcal{D}_d(w_d)$ is the total dissipated power.

2.2. Example

Consider the RLC circuit in figure 1 described as follows. For the inductance L , the state and the

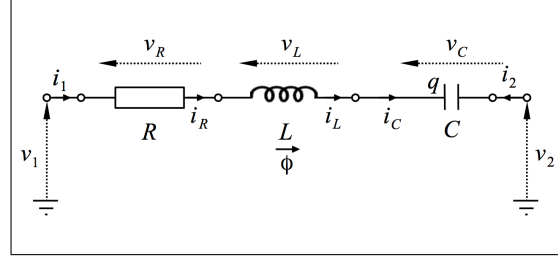


Fig. 1: RLC circuit (notations and orientations).

positive definite function can be the magnetic flux $x_1 = \phi$ and $h_1(\phi) = \phi^2/(2L)$ so that $v_L = dh_1/dx_1$ and $i_L = dx_1/dt$. For the capacitance and the resistance, quantities are defined as above with $x_2 = q$ and $\mathbf{w} = w_1 = i_R$. Port variables are arranged as input $\mathbf{u} = [v_1, v_2]^T$ and output $\mathbf{y} = [i_1, i_2]^T$. Applying Kirchhoff's laws to this simple serial circuit yields

$$\begin{pmatrix} v_L \\ i_C \\ i_R \\ i_1 \\ i_2 \end{pmatrix} = \begin{pmatrix} 0 & -1 & -1 & +1 & -1 \\ +1 & 0 & 0 & 0 & 0 \\ +1 & 0 & 0 & 0 & 0 \\ +1 & 0 & 0 & 0 & 0 \\ -1 & 0 & 0 & 0 & 0 \end{pmatrix} \cdot \begin{pmatrix} i_L \\ v_C \\ v_R \\ v_1 \\ v_2 \end{pmatrix}.$$

From the constitutive laws of components, this equation exactly restores the form (1), block by block. It provides the algebro-differential equations that govern the system with input \mathbf{u} and output \mathbf{y} .

Remark 2.1. PHS [5, 6] are not restricted to the “classical Hamiltonian systems” (CHS) [8], for which $n_D = 0$, n_S is even and \mathbf{J}_x is similar to $\mathbf{J}_x^* = \begin{pmatrix} \mathbb{0}_{n_S/2} & -\mathbb{I}_{n_S/2} \\ \mathbb{I}_{n_S/2} & \mathbb{0}_{n_S/2} \end{pmatrix}$ for symplectic coordinates. For PHS, \mathbf{J}_x can even be rank deficient: removing the capacitor (or the inductor) in figure 1 still yields (1) with $n_S = 1$ and $\mathbf{J}_x = \emptyset$. However, PHS and CHS can coincide for conservative systems ($n_D = 0$) with $n_S/2$ components that store kinetic energy and $n_S/2$ that store potential energy: removing the resistor and closing the circuit ($n_P = 0$) in figure 1 yields $n_S = 2$ and $\frac{dx}{dt} = \mathbf{J}_x^* \cdot \nabla \mathcal{H}(\mathbf{x})$.

2.3. Passivity property

The following property holds.

Property 2.1 (Power Balance). *The total energy $\mathfrak{E} = \mathcal{H}(\mathbf{x})$ of a system governed by (1) is such that*

$$\frac{d\mathfrak{E}}{dt} = \mathcal{P} - \mathcal{D}, \quad (2)$$

where $\mathcal{P} = \mathbf{u}^T \mathbf{y}$ (incoming power, external sources), and $\mathcal{D} = \mathbf{z}(\mathbf{w})^T \mathbf{w} \geq 0$ (total dissipated power).

Proof. Rewrite (1) as $\mathbf{a} = \mathbf{M} \cdot \mathbf{b}$. By definition of \mathfrak{E} , \mathcal{P} and \mathcal{D} , we have $\frac{d\mathfrak{E}}{dt} + \mathcal{D} - \mathcal{P} = \mathbf{b}^T \mathbf{\Lambda} \cdot \mathbf{a}$ with $\mathbf{\Lambda} = \text{diag}(\mathbb{I}_{n_S}, \mathbb{I}_{n_D}, -\mathbb{I}_{n_P})$. Moreover, from (1), $\mathbf{b}^T \mathbf{\Lambda} \cdot \mathbf{a} = \mathbf{b}^T \mathbf{\Lambda} \cdot \mathbf{M} \cdot \mathbf{b}$ is zero since $\mathbf{\Lambda} \cdot \mathbf{M}$ is skew-symmetric. \square

In electronics, this property is known as the *Tellegen's theorem* [7]. More generally, this property proves the *passivity* of (1) in the sense of *dynamical systems* [9, def. 6.3], recalled below.

Definition 2.1 (Passive input/output system). *A system with input \mathbf{u} , state \mathbf{x} and output \mathbf{y} is said to be passive if there exists a continuously differentiable positive semidefinite function $\mathcal{V}(\mathbf{x})$ (called a storage function) so that $\frac{d\mathcal{V}(\mathbf{x})}{dt} \leq \mathbf{y}^T \mathbf{u}$. Moreover, if $\frac{d\mathcal{V}(\mathbf{x})}{dt} \leq -\psi(\mathbf{x}, \mathbf{u}) + \mathbf{y}^T \mathbf{u}$ for some positive semidefinite function ψ , the system is said to be strictly passive.*

When the excitation stops ($\mathbf{u} = \mathbf{0}$), the positive storage function \mathcal{V} stops increasing (passive system), and decreases for strictly passive system as long as $\psi(\mathbf{x}, \mathbf{0}) > 0$. Moreover, since \mathcal{V} is continuous and definite, if \mathcal{V} decreases towards 0, then \mathbf{x} also tends towards $\mathbf{0}$ (Lyapunov asymptotic stability).

PHS (1) proves passive ($\mathcal{V} \equiv \mathcal{H}$). Moreover, if there exists a unique function \mathcal{F} such that

$$\mathcal{F}(\mathbf{x}, \mathbf{u}) = \mathbf{K}^T \cdot \nabla \mathcal{H}(\mathbf{x}) + \mathbf{J}_w \cdot \mathbf{z}(\mathcal{F}(\mathbf{x}, \mathbf{u})) + \mathbf{G}_w \cdot \mathbf{u}, \quad (3)$$

then $\psi(\mathbf{x}, \mathbf{u}) = \mathcal{D}(\mathbf{x}, \mathbf{u}) = \mathbf{z}^T(\mathcal{F}(\mathbf{x}, \mathbf{u})) \cdot \mathcal{F}(\mathbf{x}, \mathbf{u})$. A sufficient condition on \mathbf{z} is given below.

Proposition 2.1. *$\mathcal{F}(\mathbf{x}, \mathbf{u})$ exists and is unique if \mathbf{z} is injective and its Jacobian matrix $\mathcal{J}_z(\mathbf{w})$ is positive definite for all \mathbf{w} .*

Proof. If $\mathcal{G}(\mathbf{w}) = \mathbf{w} - \mathbf{J}_w \cdot \mathbf{z}(\mathbf{w})$ is invertible, then \mathcal{F} in equation (3) is given by $\mathcal{F}(\mathbf{x}, \mathbf{u}) = \mathcal{G}^{-1}(\mathbf{K}^T \cdot \nabla \mathcal{H}(\mathbf{x}) + \mathbf{G}_w \cdot \mathbf{u})$. This is true from the global inverse function theorem if \mathcal{G} is injective and its jacobian matrix is always invertible. Indeed, since \mathbf{J}_w is skew-symmetric, $\mathcal{G}(\mathbf{w}_1) - \mathcal{G}(\mathbf{w}_2) = \mathbf{0}$ implies $(\mathbf{z}(\mathbf{w}_1) - \mathbf{z}(\mathbf{w}_2))^T \cdot (\mathbf{w}_1 - \mathbf{w}_2) = 0$, and thus \mathcal{G} is injective if \mathbf{z} is injective. If additionally $\mathcal{J}_z(\mathbf{w})$ is positive definite, $\mathcal{X}^T \mathcal{J}_z(\mathbf{w})^T \cdot (\mathbb{I}_{n_D} - \mathbf{J}_w) \cdot \mathcal{X} \neq 0_{n_D}$ for all vector $\mathcal{X} \neq \mathbf{0}_{n_D}$, so that $\mathcal{J}_{\mathcal{G}}(\mathbf{w})$ is invertible. \square

This paper aims to simulate such passive systems by deriving numerical version of (1) so that a numerical version of the power balance (2) is satisfied and the Lyapunov stability is preserved.

3. CIRCUIT UNDER CONSIDERATION

The method is applied in this paper on the Cry-Baby wah pedal, whose schematic is given in figure 3. First, the network is analysed in the meaning of the graph theory. Second, a dictionary of some elementary components is built.

3.1. Network analysis

An oriented graph is defined by a set \mathbf{N} of n_N nodes and a set \mathbf{B} of n_B oriented branches. Such objects are described by their incidence matrix $\mathbf{\Gamma} \in \mathbb{R}^{n_N \times n_B}$:

$$[\mathbf{\Gamma}]_{n,b} = \begin{cases} 1 & \text{if branch } b \text{ is outgoing node } n, \\ -1 & \text{if branch } b \text{ is ingoing node } n, \\ 0 & \text{otherwise.} \end{cases}$$

A graph representation of electronic circuits is obtained defining an electric potential ε_n on each node n of the system's graph, and assigning both a potential difference v_b and a current i_b for each branch b (see convention figure 2). Then, it becomes possible to use the Kirchhoff's laws on graphs.

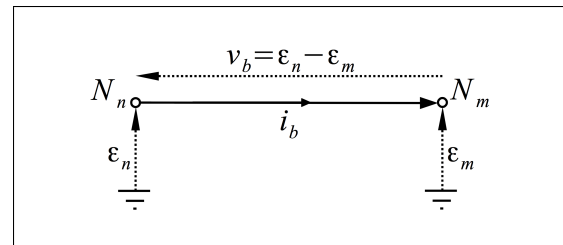
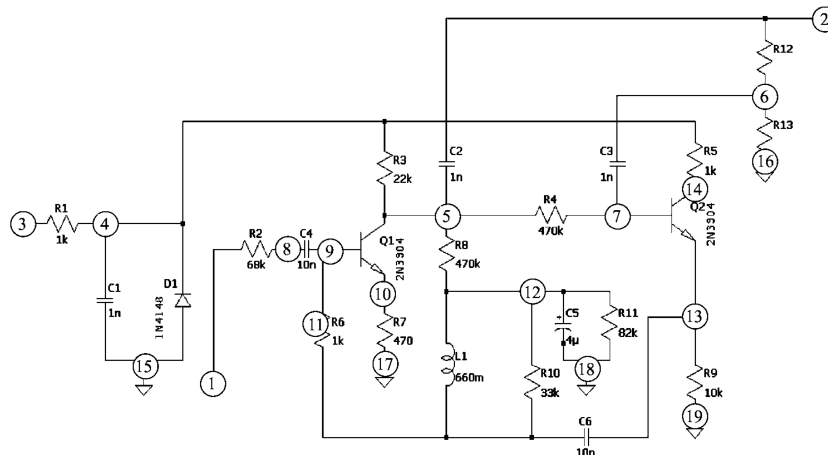


Fig. 2: Definition of potential ε , tension v and current i on a branch b going from node n to node m .



The graph of the CryBaby's circuit is made of 19 nodes (see figures 3 and 4). N_1 is the input, N_2 is the output, N_3 is the power supply and nodes N_{15} to N_{19} are connected to the ground of the circuit (that is, $u_p = v_p = 0$, $\forall p \in [15, \dots, 19]$). The branches of the network represent the components, which are described thereafter.

The dictionary is given in table 1. Note that choosing variables \mathbf{x} and \mathbf{w} as in the dictionary, matrices of the PHS (1) are canonical, that is, they do not involve any physical constants.

Storage components: Such components are defined by their storage function h associated with the constitutive laws of table 1. In this paper, all storage components are linear dipoles. The roles of $\frac{dh}{dx}$ and $\frac{dx}{dt}$ are switched for inductors and capacitors.

Resistors: The characteristics of dissipative components are algebraic relations on \mathbf{w} . Note that one differentiates the *resistive* and the *reactive* cases (see table 1).

Diodes: PN junctions are modeled as reactive components by the Shockley equation. As in SPICE simulators, a minimal conductance G_{min} is added to help convergence in the simulation process. This avoids zero values in the computation of the gradient for low values. I_S is

the saturation current, μ is an ideality factor and v_0 the reference tension, specified for each diode type. Note that the passivity property is fulfilled ($\mathbf{z}_D(\mathbf{w}_D)^T \mathbf{w}_D \geq 0$).

Transistors: NPN junctions are passive 3-ports ($\mathcal{P}_Q = \mathcal{D}_Q = \varepsilon_B \cdot i_B + \varepsilon_C \cdot i_C + \varepsilon_E \cdot i_E \geq 0$). In this paper, we use the standard Ebers-Moll model which preserves this passivity property. It is described by:

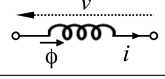
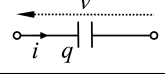
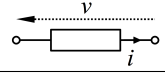
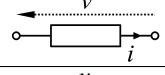
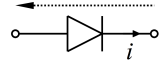
$$\begin{aligned} i_C &= I_S (e^{v_{BE}/v_t} - e^{v_{BC}/v_t}) - \frac{I_S}{\beta_R} (e^{v_{BC}/v_t} - 1), \\ i_B &= \frac{I_S}{\beta_F} (e^{v_{BE}/v_t} - 1) - \frac{I_S}{\beta_R} (e^{v_{BC}/v_t} - 1), \\ i_E &= I_S (e^{v_{BC}/v_t} - e^{v_{BE}/v_t}) - \frac{I_S}{\beta_F} (e^{v_{BE}/v_t} - 1), \end{aligned}$$

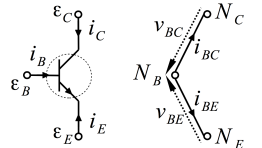
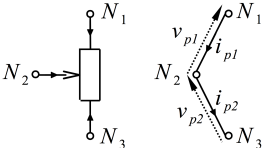
where I_S is the saturation current, β_R and β_F are respectively the reverse and forward common emitter current gains and v_t is the thermal voltage. As for the diode, minimal conductances are included. The corresponding dissipative characteristic $\mathbf{z}_Q(\mathbf{w}_Q)=[i_{BC}, i_{BE}]^T$ is given in table 1, denoting $\alpha_R = \frac{\beta_R+1}{\beta_R}$ and $\alpha_F = \frac{\beta_F+1}{\beta_F}$. The dissipated power is $\mathbf{z}_Q(\mathbf{w}_Q)^T \cdot \mathbf{w}_Q = q_1 + q_2 + q_3$ with

$$\begin{aligned} q_1 &= \frac{I_S \cdot v_{BC}}{\beta_R} \cdot (e^{v_{BC}/v_t} - 1) + \frac{I_S \cdot v_{BE}}{\beta_F} \cdot (e^{v_{BE}/v_t} - 1), \\ q_2 &= I_S \cdot (v_{BC} - v_{BE}) \cdot (e^{v_{BC}/v_t} - e^{v_{BE}/v_t}), \\ q_3 &= G_{min} \cdot ((v_{BC} - v_{BE})^2 + \frac{v_{BC}^2}{\beta_R} + \frac{v_{BE}^2}{\beta_F}), \end{aligned}$$

which proves to be non-negative. The incidence

Table 1: *Dictionary of elementary components.*

2-ports					
Storage	Diagram	x	$h(x)$	Voltage v	Current i
Inductance		ϕ	$\frac{\phi^2}{2L}$	$\frac{d\phi}{dt}$	$\frac{dh}{d\phi}$
Capacitance		q	$\frac{q^2}{2C}$	$\frac{dh}{dq}$	$\frac{dq}{dt}$
Dissipative	Diagram	w	$z(w)$	Voltage v	Current i
Resistance		i	$R.i$	$z(w)$	w
Reactance		v	v/R	w	$z(w)$
PN Diode		v	$I_S \left(\exp \left(\frac{v}{\mu v_0} \right) - 1 \right) + v.G_{min}$	w	$z(w)$

3-ports			
Dissipative	Diagram	\mathbf{w}	$\mathbf{z}(\mathbf{w})$
NPN Transistor		$\begin{pmatrix} v_{BC} \\ v_{BE} \end{pmatrix}$	$\begin{pmatrix} i_{BC} \\ i_{BE} \end{pmatrix} = \begin{pmatrix} \alpha_R & -1 \\ -1 & \alpha_F \end{pmatrix} \cdot \begin{pmatrix} I_S (e^{v_{BC}/v_t} - 1) + v_{BC}.G_{min} \\ I_S (e^{v_{BE}/v_t} - 1) + v_{BE}.G_{min} \end{pmatrix}$
Potentiometer		$\begin{pmatrix} v_{p1} \\ v_{p2} \end{pmatrix}$	$\begin{pmatrix} i_{p1} \\ i_{p2} \end{pmatrix} = \begin{pmatrix} v_{p1}/(1 + \alpha.R_p) \\ i_{p2}.(1 + (1 - \alpha).R_p) \end{pmatrix}$

matrix for a transistor is

$$\gamma_Q = \begin{pmatrix} B_{BC} & B_{BE} \\ 1 & 1 \\ -1 & 0 \\ 0 & -1 \end{pmatrix} \begin{pmatrix} N_B \\ N_C \\ N_E \end{pmatrix}.$$

Potentiometer: This component is modeled as two time-varying resistors, the sum of which is R_p . To avoid 0 value of the resistors, 1Ω have been added to those characteristics. The modulation parameter is $\alpha \in [0, 1]$. We choose B_{p1} as a conductance, and B_{p2} as a resistance, so that $\mathbf{w}_P = [v_{p1}, i_{p2}]^T$ (see table 1).

The incidence matrix for a potentiometer is

$$\gamma_P = \begin{pmatrix} B_{p1} & B_{p2} \\ 1 & 0 \\ -1 & 1 \\ 0 & -1 \end{pmatrix} \begin{pmatrix} N_1 \\ N_2 \\ N_3 \end{pmatrix}.$$

Remark 3.1. *For the nonlinear components, some resistors are added to model the resistance of contacts. For sake of simplicity, they do not appear in this paper. However, they are included in our final simulation, choosing the same values as in the LT-Spice models.*

The circuit of figures 3 is composed of 6 capacitors and 1 inductor organised as $\mathbf{B}^s = \{C_1, \dots, C_6, L_1\}$

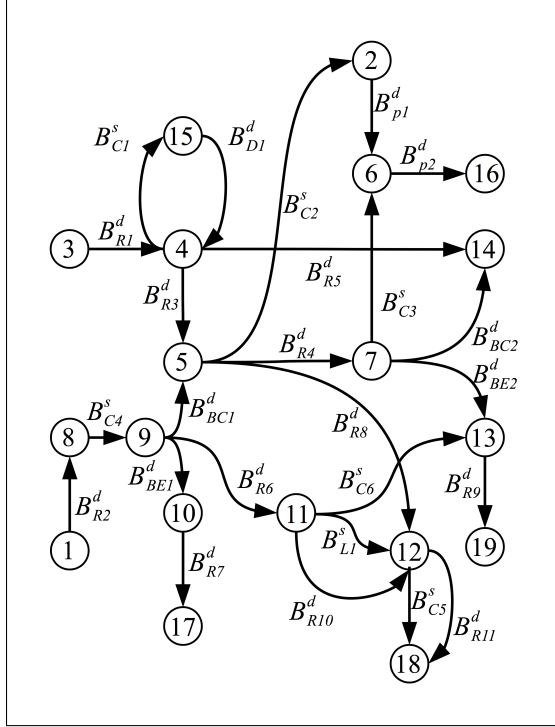


Fig. 4: Equivalent graph of the CryBaby's circuit.

($n_S=7$); 11 resistors, 1 PN diode, 2 NPN transistors and a potentiometer ($n_D = 18$) organised as $\mathbf{B}^d = \{R_1, \dots, R_{11}, D, Q_1, Q_2, P\}$; and $n_P=3$ ports (input/output signals and battery). Using the dictionary, this circuit is formulated as the graph in figure 4. The difficulty here remains in the choice of variables which are adapted to realize the system (see [6, sec.2.4.5]). We choose resistors $R_1, R_4, R_8, R_9, R_{10}$ and R_{11} as conductances, and the other ones as resistances. Thus, the sets of PHS variables are:

$$\begin{aligned} \dot{\mathbf{x}} &= [i_{C1}, \dots, i_{C6}, v_{L1}]^T, \\ \nabla \mathcal{H}(\mathbf{x}) &= [v_{C1}, \dots, v_{C6}, i_{L1}]^T, \end{aligned}$$

$$\begin{aligned} \mathbf{w} &= [\{i, v\}_R | v_d | v_{BC1}, v_{BE1} | v_{BC2}, v_{BE2} | v_{p1}, i_{p2}]^T, \\ \mathbf{z}(\mathbf{w}) &= [\{v, i\}_R | i_d | i_{BC1}, i_{BE1} | i_{BC2}, i_{BE2} | i_{p1}, v_{p2}]^T, \end{aligned}$$

where $\{i, v\}_R$ is the set of w_R and $\{v, i\}_R$ the set of $z_R(w_R)$ according to each resistor's type, and

$$\begin{aligned} \text{Inputs } \mathbf{u} &= [v_{in}, i_{out}, v_{cc}]^T, \\ \text{Outputs } \mathbf{y} &= [i_{in}, v_{out}, i_{cc}]^T. \end{aligned}$$

4. DERIVATION OF THE PHS

We proceed in two steps, as for the example in §2.2. First, we establish the matrices of PHS (1). Second, we replace each physical quantity using the adequate constitutive laws. The difficulty here remains in the first step. The method is illustrated on the simple system of figure 5, whose net-list is:

$$\begin{aligned} \text{C: } &N_1, N_2 \\ \text{L: } &N_2, N_3 \\ \text{R: } &N_2, N_4. \end{aligned}$$

This is achieved as follows. We firstly need to construct the unconnected incidence matrix $\tilde{\gamma}$, by concatenating the incidence matrices of elementary components. Recall that incidence matrix for 2-ports with convention that the current goes from N_1 to N_2 is

$$\gamma_{2\text{-port}} = \begin{pmatrix} B \\ 1 \\ -1 \end{pmatrix} \begin{matrix} N_1 \\ N_2 \end{matrix}.$$

Thus, the unconnected incidence matrix for the system of figure 5 is

$$\tilde{\gamma} = \begin{pmatrix} B_1 & B_2 & B_3 \\ 1 & \vdots & \vdots \\ -1 & \vdots & \vdots \\ \vdots & 1 & \vdots \\ \vdots & -1 & \vdots \\ \vdots & \vdots & 1 \\ \vdots & \vdots & -1 \end{pmatrix} \begin{matrix} \tilde{N}_1 \\ \tilde{N}_2 \\ \tilde{N}_2 \\ \tilde{N}_3 \\ \tilde{N}_2 \\ \tilde{N}_4 \end{matrix}.$$

Then, rows having same node label are summed together to form the actual incidence matrix:

$$\gamma = \begin{pmatrix} B_1 & B_2 & B_3 \\ 1 & \vdots & \vdots \\ -1 & 1 & 1 \\ \vdots & -1 & \vdots \\ \vdots & \vdots & -1 \end{pmatrix} \begin{matrix} N_1 \\ N_2 \\ N_2 \\ N_3 \\ N_4 \end{matrix}.$$

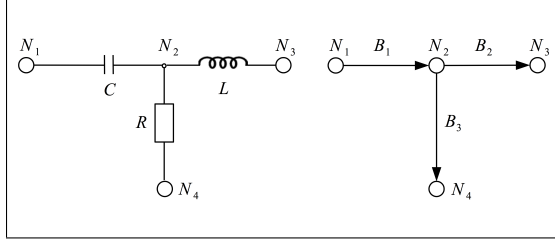


Fig. 5: Equivalent graph representation of an RLC system: $B_1 \leftrightarrow C$, $B_2 \leftrightarrow L$ and $B_3 \leftrightarrow R$.

Input/output quantities are introduced by defining a (virtual) reference node N_0 (see figure 6), and the set of *port branches* $\mathbf{B}^p = \{B_1^p, \dots, B_{n_P}^p\}$. The circuit branches are sorted by type (storage, dissipative and then port branches) and by linearity for components (linear and then non-linear constitutive laws). Note that the total number of branches n_B is the sum $n_S + n_D + n_P$ of the number of storage branches, dissipative branches and port branches. In the receiver convention, the total incidence ma-

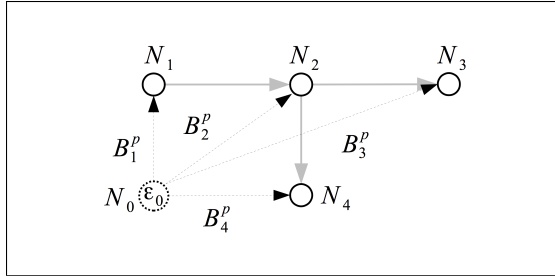


Fig. 6: Introducing reference node N_0 and port branches \mathbf{B}^p in the graph of figure 5.

trix of the system is given by $\mathbf{\Gamma} = [\boldsymbol{\gamma}, \boldsymbol{\gamma}_p] \in \mathbb{R}^{n_N \times n_B}$ where element (n, b) of $\boldsymbol{\gamma}_p \in \mathbb{R}^{n_N \times n_P}$ is -1 if the port branch b is connected to node n , 0 otherwise. Defining $\mathbf{v} = [\mathbf{v}_s, \mathbf{v}_d, \mathbf{v}_p]^T \in \mathbb{R}^{n_B}$ the branches tensions, $\mathbf{i} = [\mathbf{i}_s, \mathbf{i}_d, \mathbf{i}_p]^T \in \mathbb{R}^{n_B}$ the branches currents, and $\boldsymbol{\varepsilon} = \{\varepsilon_1, \dots, \varepsilon_{n_N}\}$ the set of the potentials on the (real) nodes of the system, the Kirchhoff voltage law can be expressed as $\mathbf{v} = \mathbf{\Gamma}^T \boldsymbol{\varepsilon}$, and the Kirchhoff's current law as $\mathbf{\Gamma} \mathbf{i} = \mathbf{0}$. Hence, passivity of the system is guaranteed if the following set of relations is true all the time:

$$\begin{pmatrix} \mathbf{v} \\ \mathbf{0} \end{pmatrix} = \begin{pmatrix} \mathbf{\Gamma}^T & \mathbf{0} \\ \mathbf{0} & \mathbf{\Gamma} \end{pmatrix} \cdot \begin{pmatrix} \boldsymbol{\varepsilon} \\ \mathbf{i} \end{pmatrix}. \quad (4)$$

Note that the Tellegen's theorem can be expressed as $\mathbf{v}^T \cdot \mathbf{i} = 0$, and thus $\mathbf{v}_p^T \cdot \mathbf{i}_p = -\mathcal{P}$ is the power of the sources in emitter convention. To take it in consideration, the tensions on port branches \mathbf{B}^p are considered in the opposite way. The equivalent PHS formulation of the graph of the circuit is derived by defining $\tilde{\mathbf{x}} = [\mathbf{v}, \boldsymbol{\varepsilon}, \mathbf{i}]^T$ and rewriting equation (4) as

$$\underbrace{\begin{bmatrix} -\mathbb{I}_{n_B} & \mathbf{\Gamma}^T & \mathbf{0} \\ \mathbf{0} & \mathbf{0} & \mathbf{\Gamma} \end{bmatrix}}_{\tilde{\mathbf{\Gamma}}} \tilde{\mathbf{x}} = \mathbf{0}_{n_N + n_B}.$$

Then, the quantities are reorganized through the permutation Π , to build the vector $\tilde{\mathbf{x}} = \Pi[\tilde{\mathbf{x}}] = [\dot{\mathbf{x}}, \mathbf{w}, \mathbf{y}, \nabla \mathcal{H}(\mathbf{x}), \mathbf{z}(\mathbf{w}), \mathbf{u}, \boldsymbol{\varepsilon}]^T$. The same permutation Π is applied on the row vectors of $\tilde{\mathbf{\Gamma}}$ to form $\tilde{\tilde{\mathbf{\Gamma}}}$. Finally, the node potentials are eliminated using the Gauss-Jordan elimination algorithm on the relation $\tilde{\tilde{\mathbf{\Gamma}}} \tilde{\mathbf{x}} = \mathbf{0}$, in order to obtain $[\dot{\mathbf{x}}, \mathbf{w}, \mathbf{y}]^T$ as the (looked for) linear combination of $[\nabla \mathcal{H}(\mathbf{x}), \mathbf{z}(\mathbf{w}), \mathbf{u}]^T$.

5. SIMULATION

In this section, a numerical scheme is specially designed so that a numerical time version of the power balance (2) is satisfied.

5.1. Discrete-time version of the power balance

A numerical approximation of equation (2) is $\delta_t \mathcal{E}(k) = \mathcal{P}(k) - \mathcal{D}(k)$, where k denotes the sample number, δT is the sampling period and $\delta_t \mathcal{E}(k) = \frac{\mathcal{E}(k+1) - \mathcal{E}(k)}{\delta T}$ is a finite difference scheme. $\mathcal{E} = \mathcal{H}(\mathbf{x})$ is a composed function of time. This leads to introduce the discrete hamiltonian gradient so that $[\delta_{\mathbf{x}} \mathcal{H}(\mathbf{x}, \delta \mathbf{x})]_s = \frac{h_s[x_s(k) + \delta x_s(k)] - h_s[x_s(k)]}{\delta x_s(k)}$, where $\delta x_s(k) = x_s(k+1) - x_s(k)$, $\forall s \in [1 \dots n_S]$. Specially designed numerical scheme preserving the stability for solving equation (2) is given by:

$$\delta_t \mathcal{E}(k) = [\delta_{\mathbf{x}} \mathcal{H}(\mathbf{x}, \delta \mathbf{x})]^T \cdot \delta_t \mathbf{x}(k)$$

where $\delta_t \mathbf{x}(k) = \frac{\mathbf{x}(k+1) - \mathbf{x}(k)}{\delta T}$. Hence, placing the sample number in subscript, a numerical version of system (1) preserving the passivity is given by

$$\begin{aligned} \frac{\mathbf{x}_{k+1} - \mathbf{x}_k}{\delta T} &= \mathbf{J}_x \cdot \delta_{\mathbf{x}} \mathcal{H}(\mathbf{x}, \delta \mathbf{x}) - \mathbf{K} \cdot \mathbf{z}(\mathbf{w}_k) + \mathbf{G}_x \cdot \mathbf{u}_k \\ \mathbf{w}_k &= \mathbf{K}^T \cdot \delta_{\mathbf{x}} \mathcal{H}(\mathbf{x}, \delta \mathbf{x}) + \mathbf{J}_w \cdot \mathbf{z}(\mathbf{w}_k) + \mathbf{G}_w \cdot \mathbf{u}_k \\ \mathbf{y}_k &= \mathbf{G}_x^T \cdot \delta_{\mathbf{x}} \mathcal{H}(\mathbf{x}, \delta \mathbf{x}) + \mathbf{G}_w^T \cdot \mathbf{z}(\mathbf{w}_k) + \mathbf{J}_y \cdot \mathbf{u}_k \end{aligned} \quad (5)$$

System (5) is implicit on \mathbf{x}_{k+1} and \mathbf{w}_k . This point is discussed thereafter.

5.2. Linear storage components case

Given the constitutive laws of table 1, the (locally) stored energy is $h_s(x_s) = x_s^2/(2C_s)$ for $s \in [1 \cdots n_S]$, with C_s the linear characteristic of the s -th storage component (C_s is a capacitance or an inductance), and $\delta_{x_s} h_s(x_{s,k}, \delta x_{s,k}) = \frac{1}{2C_s} \cdot \frac{x_{s,k+1}^2 - x_{s,k}^2}{x_{s,k+1} - x_{s,k}}$. Hence, defining $\mathbf{Q}_x = \text{diag}[C_1^{-1}, \dots, C_{n_S}^{-1}]$, the numerical gradient of the Hamiltonian is $\delta_{\mathbf{x}} \mathcal{H}(\mathbf{x}, \delta \mathbf{x}) = \frac{1}{2} \mathbf{Q}_x [\mathbf{x}_{k+1} + \mathbf{x}_k]$, and thus the system to solve is

$$\begin{aligned} \mathbf{x}_{k+1} &= \mathbf{A}_x \cdot \mathbf{B}_x \cdot \mathbf{x}_k + \delta T \cdot \mathbf{A}_x \cdot [\mathbf{G}_x \cdot \mathbf{u}_k - \mathbf{K} \cdot \mathbf{z}(\mathbf{w}_k)] \\ \mathbf{w}_k &= \mathbf{A}_w \cdot \mathbf{x}_k + \mathbf{B}_w \cdot \mathbf{z}(\mathbf{w}_k) + \mathbf{C}_w \cdot \mathbf{u}_k \\ \mathbf{y}_k &= \mathbf{A}_y \cdot \mathbf{x}_k + \mathbf{B}_y \cdot \mathbf{z}(\mathbf{w}_k) + \mathbf{C}_y \cdot \mathbf{u}_k \end{aligned},$$

with

$$\mathbf{A}_x = (\mathbb{I}_{n_S} - (\delta T/2) \cdot \mathbf{J}_x \cdot \mathbf{Q}_x)^{-1} \quad (6)$$

$$\mathbf{B}_x = \mathbb{I}_{n_S} + (\delta T/2) \cdot \mathbf{J}_x \cdot \mathbf{Q}_x \quad (7)$$

$$\mathbf{A}_w = (1/2) \cdot \mathbf{K}^T \cdot \mathbf{Q}_x \cdot (\mathbb{I}_{n_S} + \mathbf{A}_x \cdot \mathbf{B}_x) \quad (8)$$

$$\mathbf{B}_w = \mathbf{J}_w - (\delta T/2) \cdot \mathbf{K}^T \cdot \mathbf{Q}_x \cdot \mathbf{A}_x \cdot \mathbf{K} \quad (9)$$

$$\mathbf{C}_w = \mathbf{G}_w + (\delta T/2) \cdot \mathbf{K}^T \cdot \mathbf{Q}_x \cdot \mathbf{A}_x \cdot \mathbf{G}_x \quad (10)$$

$$\mathbf{A}_y = (1/2) \cdot \mathbf{G}_x \cdot \mathbf{Q}_x \cdot (\mathbb{I}_{n_S} + \mathbf{A}_x \cdot \mathbf{B}_x) \quad (11)$$

$$\mathbf{B}_y = \mathbf{G}_w - (\delta T/2) \cdot \mathbf{G}_x \cdot \mathbf{Q}_x \cdot \mathbf{A}_x \cdot \mathbf{K} \quad (12)$$

$$\mathbf{C}_y = \mathbf{J}_y + (\delta T/2) \cdot \mathbf{G}_x \cdot \mathbf{Q}_x \cdot \mathbf{A}_x \cdot \mathbf{G}_x^T \quad (13)$$

Remark 5.1. *The dimension of the dissipative part of the system can be significantly reduced by distributing the relations involving linear dissipative components on the structure matrices.*

System (6) is still implicate on \mathbf{w}_k , so one uses the Newton-Raphson algorithm to approximate the dissipative state value.

5.3. Newton-Raphson method

Newton-Raphson method can be summarized as follows. The nearest root \mathbf{w}_k^* of a function $\mathbf{f} : \mathbf{w}_k \in \mathbb{R}^{n_D} \rightarrow \mathbf{f}(\mathbf{w}_k) \in \mathbb{R}^{n_D}$ (so that $\mathbf{f}(\mathbf{w}_k^*) = \mathbf{0}$) is iteratively approximated by the following algorithm:

$$\mathbf{w}_{k,n+1} = \mathbf{w}_{k,n} - \mathcal{J}_{\mathbf{f}}(\mathbf{w}_{k,n})^{-1} \cdot \mathbf{f}(\mathbf{w}_{k,n})$$

with $\mathcal{J}_{\mathbf{f}}(\cdot)$ the Jacobian matrix of \mathbf{f} . In the present case: $\mathbf{f}(\mathbf{w}_k) = \mathbf{w}_k - \mathbf{B}_w \cdot \mathbf{z}(\mathbf{w}_k) - \underbrace{(\mathbf{A}_w \mathbf{x}_k + \mathbf{C}_w \mathbf{u}_k)}_{\mathbf{C}_k}$.

5.4. Simulation algorithm

Denoting by \mathcal{T} the number of time-steps and \mathcal{N} the number of Newton-Raphson iterations per time-step, the simulation algorithm is given thereafter:

compute equations 6 to 13

$\mathbf{x}_1 \leftarrow \mathbf{0}_{n_S}$

$\mathbf{w}_0 \leftarrow \mathbf{0}_{n_D}$

for $k = [1 \rightarrow \mathcal{T}]$

$\mathbf{w}_{k,1} \leftarrow \mathbf{w}_{k-1}$

$\mathbf{C}_k \leftarrow \mathbf{A}_w \cdot \mathbf{x}_k + \mathbf{C}_w \cdot \mathbf{u}_k$

for $n = [1 \rightarrow \mathcal{N}]$

$\mathbf{f}(\mathbf{w}_{k,n}) \leftarrow \mathbf{w}_{k,n} - \mathbf{B}_w \cdot \mathbf{z}(\mathbf{w}_{k,n}) - \mathbf{C}_k$

$\mathcal{J}_{\mathbf{f}}(\mathbf{w}_{k,n}) \leftarrow \mathbb{I}_{n_D} - \mathbf{B}_w \cdot \mathcal{J}_{\mathbf{z}}(\mathbf{w}_{k,n})$

$\mathbf{w}_{k,n+1} \leftarrow \mathbf{w}_{k,n} - \mathcal{J}_{\mathbf{f}}(\mathbf{w}_{k,n})^{-1} \cdot \mathbf{f}(\mathbf{w}_{k,n})$

end for n

$\mathbf{w}_k \leftarrow \mathbf{w}_{k,\mathcal{N}+1}$

$\mathbf{y}_k \leftarrow \mathbf{A}_y \cdot \mathbf{x}_k + \mathbf{B}_y \cdot \mathbf{z}(\mathbf{w}_k) + \mathbf{C}_y \cdot \mathbf{u}_k$

$\mathbf{x}_{k+1} \leftarrow \mathbf{A}_x \cdot \mathbf{B}_x \cdot \mathbf{x}_k + \delta T \cdot \mathbf{A}_x \cdot [\mathbf{G}_x \cdot \mathbf{u}_k - \mathbf{K} \cdot \mathbf{z}(\mathbf{w}_k)]$

end for k

6. RESULTS ON THE CRYBABY'S CIRCUIT

We use the algorithm of section 5.4 with the sampling rate $\delta T^{-1} = 192\text{kHz}$, and $\mathcal{N} = 3$ Newton-Raphson iterations. Note that the *wah* parameter is the potentiometer coefficient $\alpha(k)$, $i_{out} = 0A$ and $v_{cc} = 9V$. First, we apply a guitar sample as an input on v_{in} and make the *wah* parameter continuously varying. The simulation performs well (audio examples are available here¹). Second, the input v_{in} is defined as a white noise normalised to 1V, and an equivalent LTSpice simulation of the circuit is realized. Note that LTSpice doesn't support ".wav" files at 192kHz, so the sample rate in LTSpice is $\delta T^{-1} = 44,1\text{kHz}$. The transfer functions $T_{cry} = 20 \cdot \log_{10} \frac{|TF(V_{out})|}{|TF(V_{in})|}$ are given in figure 7.

7. CONCLUSIONS

We have established a method to recast an analog audio circuit into PHS formalism, which guarantees passivity of the model. This method lies on two points: (1) the graph theory to describe a circuit network and (2) a dictionary of elementary components which are conformable with PHS theory. Then, we designed a first-order numerical scheme that preserves passivity. The whole procedure has

¹<http://recherche.ircam.fr/anasynt/falaize-skrzek/html/aes135.html>

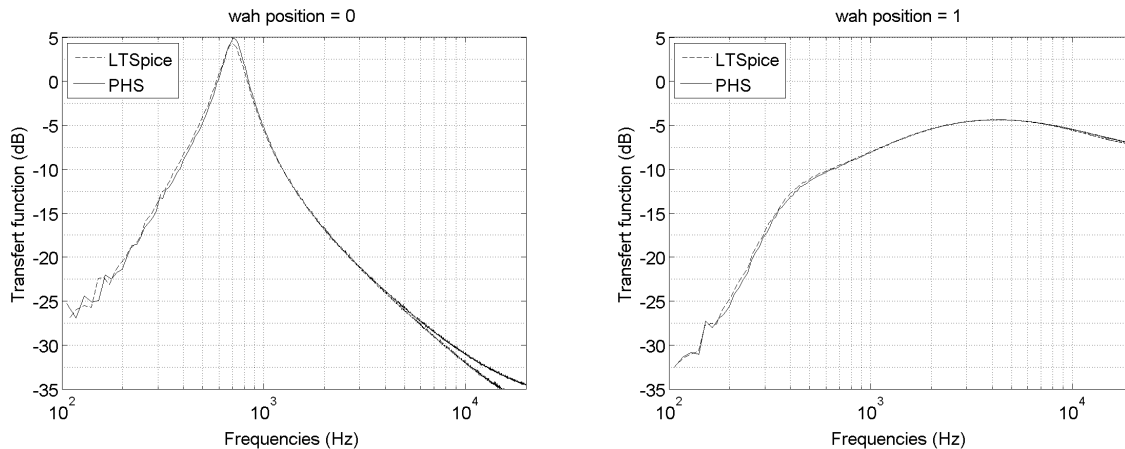


Fig. 7: Comparison of the transfer functions of LTSpice simulation and our PHS simulation of the CryBaby.

been applied to a time-varying audio circuit, the CryBaby wah pedal. Finally, our simulations are consistent with LTSpice results. One perspective for further work is to consider higher-order numerical schemes (Runge-Kutta, etc.). Another perspective is to automatically generate a SHP and its simulation code from a netlist.

8. REFERENCES

- [1] Fettweis, A. (1986). Wave digital filters: Theory and practice. *Proceedings of the IEEE*, 74(2), 270-327.
- [2] Yeh, D. T., Abel, J. S., & Smith, J. O. (2010). Automated physical modeling of nonlinear audio circuits for real-time audio effects - Part I: Theoretical development. *Audio, Speech, and Language Processing, IEEE Transactions on*, 18(4), 728-737.
- [3] Holters, M., & Zlzer, U. (2011). Physical Modelling of a WahWah Effect Pedal as a case study for Application of the nodal DK Method to circuits with variable parts. *Proc. Digital Audio Effects (DAFx-11)*, Paris, France.
- [4] Maschke, B. M., Van der Schaft, A. J., & Breedveld, P. C. (1992). An intrinsic Hamiltonian formulation of network dynamics: Non-standard Poisson structures and gyrators. *Journal of the Franklin institute*, 329(5), 923-966.
- [5] Van der Schaft, A. J. (2006). Port-Hamiltonian systems: an introductory survey. *Proceedings of the International Congress of Mathematicians (3): Invited Lectures*, 1339-1365.
- [6] Stramigioli, S., Duindam, V., & Macchelli, A. (2009). *Modeling and Control of Complex Physical Systems: The Port-Hamiltonian Approach*. Springer.

- [7] Desoer, C. A., & Kuh, E. S. (2009). *Basic circuit theory*. Tata McGraw-Hill Education.
- [8] Marsden, J. E., & Ratiu, T. S. (1999). *Introduction to mechanics and symmetry: a basic exposition of classical mechanical systems (Vol. 17)*. Springer.
- [9] Khalil, H. K. (2002). *Nonlinear systems (Vol. 3)*. Upper Saddle River: Prentice hall.

9. ACKNOWLEDGEMENT

The contribution of both authors has been done within the context of the French National Research Agency sponsored project HAMECMOPSY. Further information is available here². The PhD thesis of Antoine Falaize-Skrzek is funded by the EDITE school from Paris. The authors also wish to thank Bernhard Maschke for his introduction to PHS theory, G  rard Bertrand for his useful advices in the field of electronic circuits and Tarik Usciati for having paved the way of the present work.

²<http://www.hamecmopsys.ens2m.fr/>